Food Hydrocolloids 178 (2026) 112665

Contents lists available at ScienceDirect

Food Hydrocolloids

journal homepage: www.elsevier.com/locate/foodhyd

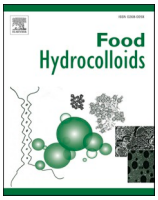

# Interfacial stabilization mechanism in one-step W/O/W multiple emulsions: The role of cellulose nanofibrils and oleic acid

Maria C.S. Oliveira [a,b], Caroline E.P. Silva [c], Elisa S. Ferreira [a], James M. Almeida [d,e], Juliana S. Bernardes [a,b,e,*]

[a] Brazilian Nanotechnology National Laboratory (LNNano), Brazilian Center for Research in Energy and Materials (CNPEM), Campinas, SP, Brazil
[b] Institute of Chemistry, University of Campinas (UNICAMP), Campinas, SP, Brazil
[c] Brazilian Synchrotron Light Laboratory (LNLS), Brazilian Center for Research in Energy and Materials (CNPEM), Campinas, SP, Brazil
[d] Ilum School of Science (Ilum), Brazilian Center for Research in Energy and Materials (CNPEM), Campinas, SP, Brazil
[e] Center of Natural and Human Sciences, Federal University of ABC (UFABC), Santo André, SP, Brazil

ARTICLE INFO

*Keywords:*
Multiple emulsion
Cationic cellulose nanofibrils
Oxidized cellulose nanofibrils
Oleic acid
Almond oil
Molecular dynamics simulation

ABSTRACT

The multiphase structure and large interfacial area of multiple emulsions have driven increasing interest in their use in the pharmaceutical, cosmetics, and food industries. However, the presence of two thermodynamically unstable interfaces remains a challenge that hinders their broader application. Typically, the production of multiple emulsions requires large amounts of synthetic emulsifiers and a two-step preparation process. Here, we developed novel almond oil $W_1/O/W_2$ multiple emulsions in one step by combining cellulose nanofibrils (CNFs) and oleic acid as bio-based emulsifiers. Cationic or anionic cellulose nanofibrils (CNFs), with average widths of about 2 nm, acted as Pickering stabilizers at the $O/W_2$ interface, producing oil droplets with diameters in the tens of micrometers. The internal $W_1/O$ emulsion, composed of water droplets a few micrometers in size, was stabilized by the naturally occurring oleic acid in the oil phase. Molecular dynamics simulations showed that increasing oleic acid content reduces the interfacial tension from 28 to 19 mN $m^{-1}$. Emulsions prepared with mineral oil as an alternative oil phase did not result in multiple emulsion formation, confirming the essential role of oleic acid in stabilizing the $W_1/O$ interface. Additionally, the stability of multiple emulsions can be tailored by the type of CNF, as electrostatic repulsion between the negatively charged CNFs and oleic acid enhances the migration of oleic acid to the $W_1/O$ interface, promoting stability for over 60 days. These results demonstrate the capability of functionalized CNFs and oleic acid in the design of multiple emulsions using a practical method, with possible use in food and cosmetic formulations.

## 1. Introduction

A water-in-oil-in-water ($W_1/O/W_2$) multiple emulsion is a complex system consisting of water droplets enclosed within oil droplets, which are further dispersed in a continuous aqueous phase. Interest in multiple emulsions has recently increased due to their ability to encapsulate both hydrophilic and hydrophobic compounds simultaneously, offering enhanced stability and controlled release of active ingredients. This versatility is attractive for potential applications in the pharmaceutical and cosmetics fields (Garti & Bisperink, 1998). In addition, multiple emulsions are of particular interest to the food industry, as they can be used to encapsulate and protect sensitive and active food components from environmental degradation, modulate the release of aromas and flavors, and enable the development of food products with reduced oil or fat content (Muschiolik, 2007).

Multiple emulsions are typically prepared in a two-step emulsification process. First, a simple water-in-oil ($W_1/O$) emulsion is prepared with a hydrophobic emulsifier. This primary emulsion is then dispersed in water containing a hydrophilic emulsifier, resulting in the formation of the $W_1/O/W_2$ multiple emulsion. In surfactant-stabilized emulsions, this approach often requires high emulsifier concentrations, especially the hydrophobic surfactant (10-30 wt%) (Garti & Bisperink, 1998; S. Clegg et al., 2016).

Alternatively, single-step emulsification methods can be employed,

* Corresponding author. Brazilian Nanotechnology National Laboratory (LNNano), Brazilian Center for Research in Energy and Materials (CNPEM), Campinas, SP, Brazil.
*E-mail address:* juliana.bernardes@lnnano.cnpem.br (J.S. Bernardes).

https://doi.org/10.1016/j.foodhyd.2026.112665
Received 9 January 2026; Received in revised form 26 February 2026; Accepted 9 March 2026
Available online 10 March 2026
0268-005X/© 2026 The Authors. Published by Elsevier Ltd. This is an open access article under the CC BY license (http://creativecommons.org/licenses/by/4.0/).

offering benefits such as improved production efficiency and eliminating the risk of destabilizing the primary emulsion that may occur during the second step of the two-step method (S. Clegg et al., 2016). Phase inversion is a common one-step approach, where emulsions are prepared near the inversion point between O/W and W/O types, but it often results in temporary multiple emulsions (Morais et al., 2009; Zhao et al., 2022). Other single-step approaches, including microfluidics and stabilization using amphiphilic block copolymers, also face challenges related to mass production, limiting their practical application (S. Clegg et al., 2016).

To formulate multiple emulsions, whether using the one-step or two-step method, synthetic surfactants are typically employed (Garti & Bisperink, 1998). However, in recent years, the use of surfactants has raised environmental concerns, including enzyme inhibition, water pollution, and limited biodegradability (Zhao et al., 2022). Moreover, the absence of surfactants is particularly advantageous for pharmaceutical and cosmetic applications, where they may trigger potential health risks, including allergic and carcinogenic reactions (Muhammad et al., 2024). As a result, there is growing interest in natural, renewable, and biocompatible stabilizers, especially those derived from plant sources (Zakir Hossain et al., 2021).

Cellulose nanofibrils (CNFs) are particles derived from biomass that have attracted interest as stabilizers for Pickering emulsions (Dufresne, 2013; Q. Li, Gong, et al., 2021). Unlike conventional emulsions stabilized by surfactants, Pickering emulsions employ colloidal solid particles that adsorb strongly at the oil–water interface, forming a physical barrier that effectively prevents droplet coalescence (Aveyard et al., 2003; Binks & Horozov, 2006, chap. 1). Due to their intrinsic hydrophilicity, cellulose nanoparticles tend to form O/W emulsions (Fujisawa et al., 2017). Silva et al. (Silva et al., 2020) demonstrated that cationic CNFs can produce O/W Pickering emulsions with remarkable long-term stability. However, more complex systems stabilized exclusively by nanocelluloses, such as multiple emulsions, remain largely unexplored (Cunha et al., 2014). Strategies to enable their application in such systems include tuning particle wettability through surface modification (e.g., hydrophobization) or by incorporating salts, surfactants, or polymers (Carrillo et al., 2015; Cunha et al., 2014).

In the search for renewable hydrophobic stabilizers for W/O emulsions, fatty acids show promise for use in these systems (Johansson & Svensson, 2001; Svensson, 2010). Their amphiphilic structure, composed of a nonpolar hydrocarbon chain and a polar carboxylic group (Hąc-Wydro & Wydro, 2007), imparts surface activity, including adsorption at water-air (Shu et al., 2014) and water-oil (Freire et al., 2022) interfaces, as well as self-assembly into aggregates (Johansson & Svensson, 2001; Svensson, 2010). Fatty acids are abundant, biocompatible, and naturally present in various oleochemical sources such as animal fats, marine oils, and vegetable oils (Johansson & Svensson, 2001; Svensson, 2010). Oleic acid is an abundant monounsaturated fatty acid and constitutes a major component of numerous vegetable oils (Choulis, 2011; Freire et al., 2022). Its application in emulsion systems has been reported in relatively few studies, primarily focusing on O/W emulsions. In these cases, oleic acid is typically used as the oil phase (Kamogawa et al., 2001, 2004; Suga et al., 2016), although some studies have utilized mixtures of oleic acid and its deprotonated form (oleate) to stabilize emulsions (Freire et al., 2022; Sieben et al., 2022). Given its high lipophilicity (HLB = 1) (Myers, 1999, chap. 11; Pasquali et al., 2008), oleic acid in its protonated form represents a promising emulsifier for W/O emulsions, highlighting an opportunity for further investigation.

The stability of emulsions is influenced by the behavior of emulsifiers at the oil-water interface and by the structural properties of the interfacial film (Niu et al., 2023). Advances in computational simulations have contributed to the molecular-level understanding of these interfaces, overcoming the limitations of traditional theoretical and experimental methods. In particular, molecular dynamics (MD) simulations are a valuable tool for studying the adsorption and organization of emulsifiers at oil-water interfaces. When combined with interfacial tension calculations, MD simulations enable the atomic-scale characterization of emulsions (de Almeida et al., 2023; Muhammad et al., 2024; Niu et al., 2023). Shi et al. (Shi et al., 2018) used this approach to compare the self-assembly behavior and the interfacial tension reduction of four representative surfactants at the oil-water interface. The integration of experimental and computational methodologies represents a promising approach for designing emulsions with tailored interfacial properties (Muhammad et al., 2024). In this context, Posocco et al. (Posocco et al., 2016) combined MD simulations with experimental data to evaluate the synergistic effects of non-ionic surfactant mixtures in stabilizing O/W emulsions.

In this study, two types of chemically modified CNFs, cationic (cCNF) and anionic (aCNF), were evaluated for the one-step production of multiple emulsions using almond oil, which has a high content of oleic acid, as the oil phase. We hypothesized that CNFs could act as hydrophilic stabilizers for oil droplets ($O/W_2$ interface), whereas naturally occurring oleic acid could act as hydrophobic stabilizers for water droplets ($W_1/O$ interface), enabling the formation of novel $W_1/O/W_2$ emulsions based entirely on renewable stabilizers. The emulsions were characterized in terms of their morphological features and stability over time, using optical and confocal microscopy techniques combined with droplet size analysis. Additionally, MD simulations were employed to gain molecular-level insight into the stabilization mechanism of water droplets within the oil droplets ($W_1/O$ interface), providing a deeper understanding of the interfacial interactions governing emulsion formation.

## 2. Experimental

### 2.1. Materials

MFC was kindly provided by Suzano SA (Aracruz/ES, Brazil). Sodium hydroxide (≥98 wt%), ethanol (≥99,5%), and hydrochloric acid (37%) were purchased from Synth (Brazil). Sodium bromide (NaBr) (≥99 wt%), glycidyl-trimethylammonium chloride (GTMAC) (≥90 wt %), and 2,2,6,6-tetramethylpiperidine 1-oxyl radical (TEMPO) (98 wt %), almond oil from Prunus Dulcis, oleic acid (90% wt.%), Nile red (100% pure), and fluorescein disodium salt (≥90 wt%) were purchased from Sigma-Aldrich. Sodium hypochlorite (NaClO) (12% w/v), and mineral oil were obtained from Dinâmica Química Contemporânea (Brazil).

### 2.2. Surface modification of MFC

#### 2.2.1. Oxidation

Anionic MFC was produced by TEMPO-mediated oxidation using sodium hypochlorite in an aqueous medium at pH 10 under stirring, as proposed by Saito et al. (Saito et al., 2007) and Isogai et al. (Isogai et al., 2011). MFC (10 g dry mass) was suspended in deionized water (1000 mL) for 24 h before the addition of TEMPO (0.16 g, 1 mmol) and NaBr (1.03 g, 10 mmol). The oxidation reaction was initiated by adding a 12% (w/v) NaClO solution (155.1 g, 25 mmol NaClO per gram of cellulose), with pH adjusted to 10 using an HCl solution (3 mol $L^{-1}$). The reaction mixture was stirred for 130 min using a mechanical stirrer at room temperature, with the pH maintained at 10 by adding a NaOH solution (0.1 mol $L^{-1}$). To stop the reaction, the pH was adjusted to 7 with an HCl solution (0.1 mol $L^{-1}$), and the anionic cellulose was washed with deionized water by centrifugation until the conductivity of the supernatant was close to that of the washing water. The content of carboxylate groups, determined by conductometric titration, was found to be 1.5 mmol $g^{-1}$.

#### 2.2.2. Cationization

The cationization reaction was carried out with GTMAC in an alkaline medium, based on the methods proposed by Zaman et al. (Zaman

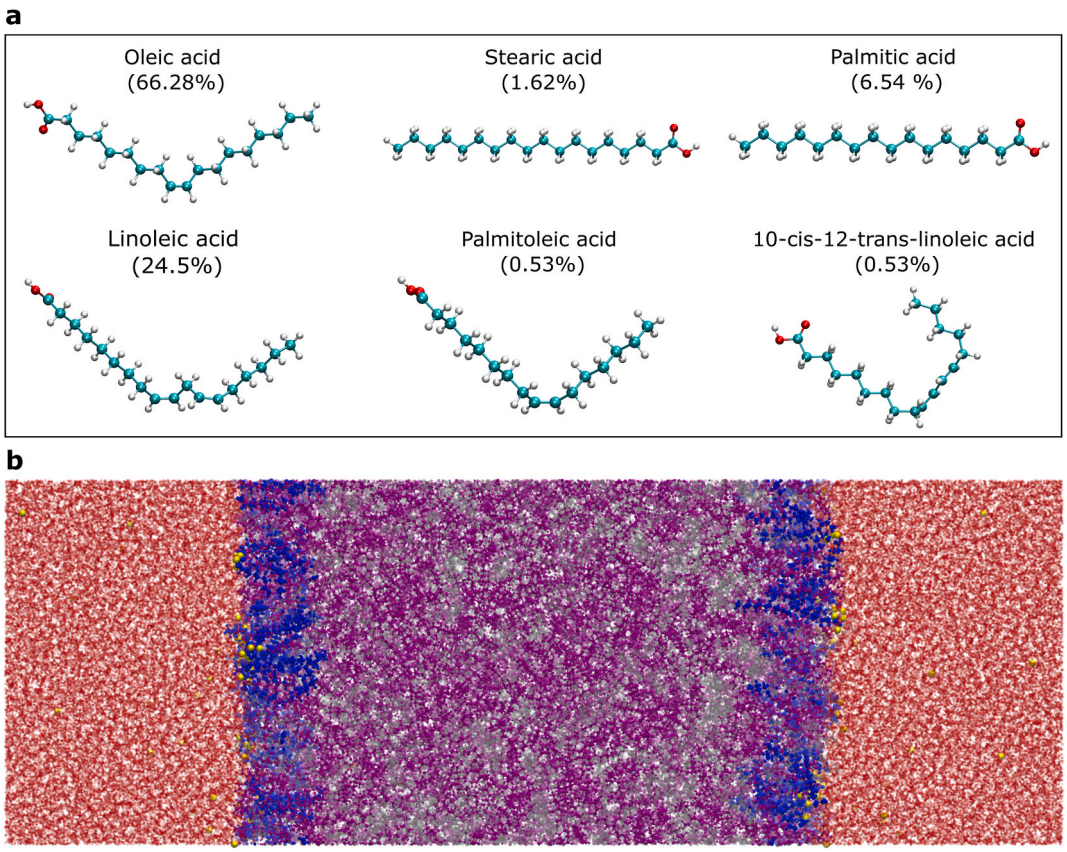


**Fig. 1.** (a) Oil model containing all molecules and concentrations. Cyan atoms are carbon, white atoms are hydrogen, and red atoms are oxygen. **(b)** Example of a simulation system with 10% deprotonation of oleic acid. Atoms are shown as spheres. Water molecules are shown in red, hydrocarbons in gray, oleic acid in purple, oleate in blue, and hydronium ions in yellow. (For interpretation of the references to colour in this figure legend, the reader is referred to the Web version of this article.)

et al., 2012). Freeze-dried MFC (10 g dry mass) was transferred to a plastic bag and NaOH (50 ml, 2.5 mol $L^{-1}$) was added dropwise. The cationic reagent GTMAC (42.08 g, 0.25 mol) was added, and the mixture was then maintained in an ultrasonic bath at 70 °C for 4 h, with manual homogenization every 30 min. At the end of the reaction, the samples were washed with 95% (v/v) ethanol solution, 0.02 mol $L^{-1}$ HCl, and deionized water and separated by centrifugation. Finally, the cationic MFC was dialyzed against deionized water for 10 days using an InLab membrane 108 (22 kDa MWCO). The amount of cationic groups in was found to be 1.1 mmol $g^{-1}$.

#### 2.2.3. Mechanical treatment

After chemical modifications, the dispersions of functionalized MFCs were diluted to 0.5 wt% and passed through a high-pressure microfluidizer (M110P, Microfluidics Corp.). Ten homogenization cycles were applied using a 200 μm chamber at a pressure of 200 bar, followed by one cycle in an 87 μm chamber at a pressure of 2000 bar, obtaining anionic CNFs (aCNF) and cationic CNFs (cCNF).

### 2.3. CNF characterization

#### 2.3.1. Atomic force microscopy (AFM)

The morphologies of CNFs were analyzed by AFM using a Bruker MultiMode microscope. Before the analysis, a droplet of the diluted suspension (20 μL, 0.0005 wt%) was deposited onto a mica substrate and dried overnight at room temperature. The samples were scanned using the tapping mode and a Nanoworld cantilever with a stiffness of 42 N $m^{-1}$ and a resonance frequency between 260 and 320 kHz. The dimensions of the fibrils were determined using the Gwyddion Software (Version 2.61) by measuring 100 independent elements.

#### 2.3.2. Zeta (ξ) potential

The ξ-potential of 0.01 wt% functionalized MFC dispersions were measured at pH 7 and 25 °C using a Zeta Sizer Ultra (Malvern Panalytical Ltd.). Each sample was subjected to three measurements.

#### 2.3.3. Scanning electron microscopy (SEM)

The morphology of cCNF and aCNF was observed by SEM using a Helios NanoLab 660 field emission gun (FEG) microscope (Thermo Fisher Scientific) in secondary electron mode, operating at 1 kV. The CNF dispersions were deposited on silicon wafers, and a carbon film with an approximate thickness of 5 nm was deposited on the samples using coating equipment (LEICA, EM ACE600) in a carbon wire evaporation method.

### 2.4. Preparation of $W_1/O/W_2$ multiple emulsions

Emulsions were produced using almond oil and CNF dispersions with an oil/water volume ratio of 40/60. The stabilizer concentration (cCNF or aCNF dispersions) in the aqueous phase was adjusted to 1 wt%. The emulsion was prepared in a single-step procedure by using a high-speed homogenizer (Ultra Turrax T10 basic IKA) for 5 min at 30,000 rpm. The emulsions were prepared using cCNF or aCNF as stabilizers under the same conditions, resulting in cCNF emulsions and aCNF emulsions, respectively.

### 2.5. $W_1/O/W_2$ multiple emulsions characterization

#### 2.5.1. Optical microscopy

The optical microscopy images of emulsions were taken by a Zeiss Axiocam ICc5 optical microscope with a magnification of 20x.

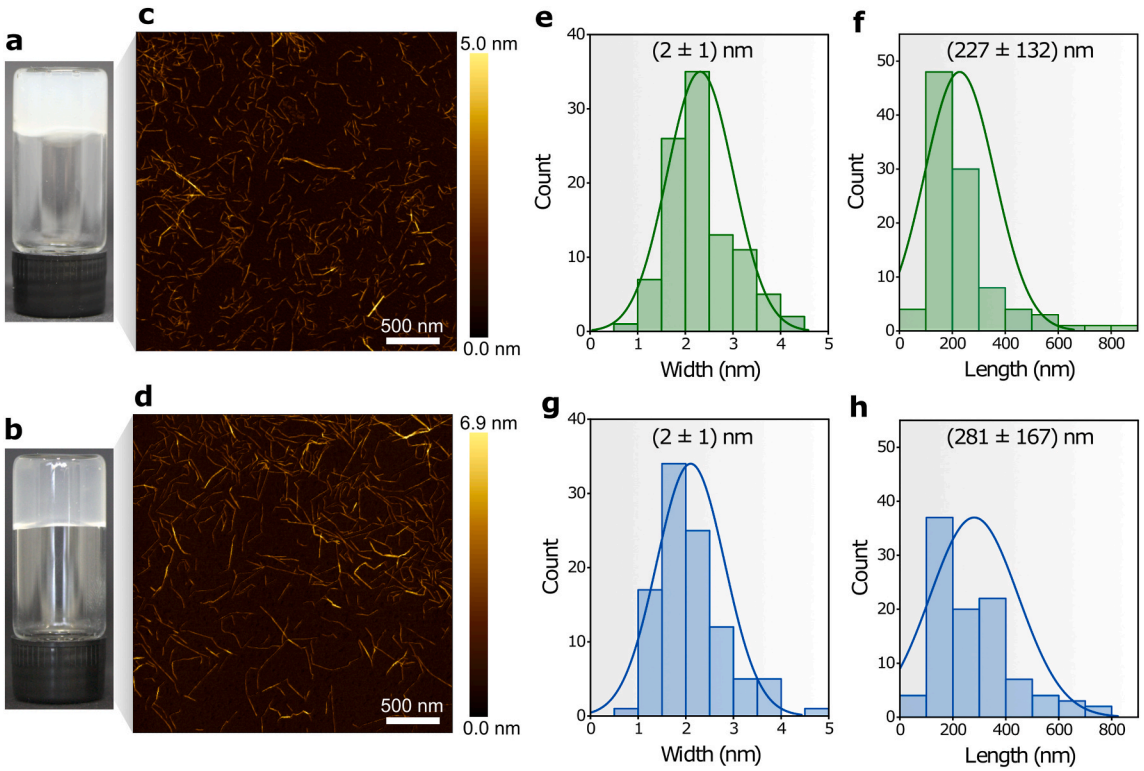


**Fig. 2.** Photographs of 1 wt% dispersion of (a) cCNF and (b) aCNF. AFM topography images of (c) cCNFs and (d) aCNFs. Width and length distribution histograms exhibiting the average and standard deviation of (e,f) cCNFs and (g,h) aCNFs.

#### 2.5.2. Confocal laser scanning microscopy (CLSM)

Prior to the emulsion preparation, water was stained with fluorescein (0.04 g $L^{-1}$) and almond oil with Nile red (0.1 g $L^{-1}$). CLSM images of the emulsions were acquired using a TCS SP8 STED 3X confocal microscope (Leica Microsystems Inc., Germany) equipped with a 63x water-immersion lens and an Ar laser at 552-636 (Nile red) and 498-517 (fluorescein). The droplet size distribution of the different emulsions were measured of 100 independent elements from their corresponding images using the software ImageJ.

#### 2.5.3. Centrifugation

To evaluate stability, the emulsions were centrifuged for 10 min at 2000 RPM (268 RCF) in an Eppendorf MiniSpin centrifuge.

### 2.6. Preparation of mineral oil emulsion

Pickering emulsions were prepared using mineral oil with an oil/water volume ratio of 40/60. The aCNF was used as the stabilizer at a concentration of 1 wt% in the aqueous phase. The emulsion was prepared in a single-step procedure by using a high-speed homogenizer (Ultra Turrax T10 basic IKA) for 5 min at 30,000 rpm.

### 2.7. Preparation of W/O emulsions

Emulsions were prepared using almond oil and oleic acid as the oil phase with an oil/water volume ratio of 99/1. Any stabilizer was added to the system. The emulsion was prepared in a single-step procedure by using a high-speed homogenizer (Ultra Turrax T10 basic IKA) for 5 min at 30,000 rpm.

### 2.8. Almond oil composition

The fatty acid composition and free fatty acids content of almond oil (Table S1) were determined according to the AOCS 2009 standard method using a capillary gas chromatograph (GC) (Agilent 68650 Series GC System) equipped with a DB-23 capillary column (Agilent, 50% cyanopropyl-methylpolysiloxane, 60 m × 0.25 mm × 0.25 μm). The chromatographic conditions were set as follows: column flow rate of 1.00 mL/min, linear velocity of 24 cm/s, detector temperature of 280 °C, and injector temperature of 250 °C. The oven temperature was programmed to start at 110 °C (held for 5 min), followed by an increase to 215 °C at a rate of 5 °C/min, and maintained at 215 °C for 24 min. Helium was used as the carrier gas, and the injection volume was 1.0 μL. Almond oil has an acidity (i.e. the free fatty acids content) of 0.10% attributed to the presence of oleic acid.

### 2.9. Classical molecular dynamics (MD)

The oil model was built based on experimental oil characterization (Table S1). Concentrations below 0.5% were not considered because the simulation cell size would result in a negligible number of molecules. Additionally, only single-chain molecules were considered; therefore, no di- or triglycerides were included in the simulations. The molecular structures and their respective concentrations can be seen in Fig. 1a.

The initial geometries and atomic charges of the molecules were calculated using ORCA (Neese, 2012, 2022) with a Hartree-Fock method and a 6-311g(d) basis-set, coupled with the Multiwfn (Lu, 2024; Lu & Chen, 2012) package, to perform the restrained electrostatic potential atomic partial charges method (RESP) (Woods & Chappelle, 2000). Classical MD simulations were performed with the Amber package (Case et al., 2023; Götz et al., 2012; Salomon-Ferrer et al., 2013). The force field used for the hydrocarbons was the Lipid21 (Dickson et al., 2022), for water, it was the TIP3P (Jorgensen et al., 1983), and Li et al. for the hydronium molecules (P. Li et al., 2015). MD simulations were performed with a timestep of 2 fs, together with the SHAKE algorithm (Miyamoto & Kollman, 1992). All the simulations had an initial minimization, an NVT thermalization for 2 ns, an NPT equilibration for 50 ns, followed by a 50 ns production run. The initial simulation box size was

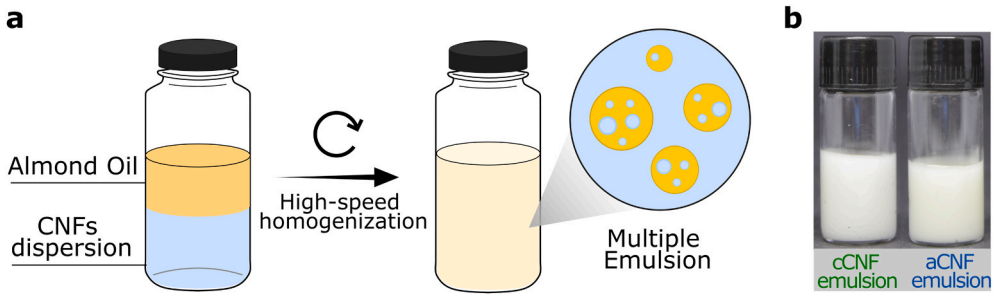


**Fig. 3.** (a) Schematic representation of the multiple emulsion preparation. (b) Photographs of freshly prepared cCNF and aCNF emulsions.

10 x 10 × 29 nm for all simulations, with approximately 179,000 atoms, and was assembled with Packmol (Martínez et al., 2009). Systems were prepared with different concentrations of deprotonated oleic acid molecules (oleate): 0%, 5%, 10%, and 20%, with hydronium ions as counter ions. Both oleate and hydronium molecules were placed at the interface during the assembly. In Fig. 1b, one of the simulations for the system containing 10% oleate is shown.

Interfacial tensions (γ) were calculated with the Irving-Kirkwood methodology (Eq. (1)) (Irving & Kirkwood, 1950), as follows:

$$\gamma = \frac{1}{2}\left(P_{zz} - \frac{1}{2}\left(P_{xx} + P_{yy}\right)\right), \quad \text{(Eq. 1)}$$

where $P_{xx}$, $P_{yy}$, and $P_{zz}$ are the diagonal components of the stress tensor. Molecular elongation was determined as the length of the elongated molecules, obtained from the ORCA optimization, minus the length observed during MD simulations. The order parameter $S_2$ was calculated according to Eq. (2) (CHAU & HARDWICK, 1998):

$$S_2 = \frac{1}{2}\left(3\cos^2\theta - 1\right), \quad \text{(Eq. 2)}$$

where θ is the angle between the molecular axis and the normal to the interface plane.

## 3. Results and discussion

### 3.1. Surface modification of the cellulose nanofibrils

In the present study, two types of functionalized CNFs, cCNFs and aCNFs, were produced to be used as Pickering stabilizers for the oil droplets of multiple emulsions. cCNFs and aCNFs were obtained through functionalization followed by mechanical disintegration of microfibrillated cellulose (MFC). The ξ-potential of cCNFs was measured at + 52.3 mV, confirming the grafting of trimethyl ammonium groups via nucleophilic substitution with GTMAC, resulting in a charged group content of 1.1 mmol/g. In contrast, aCNFs, which were functionalized with carboxylate groups through TEMPO-mediated oxidation exhibited a ξ-potential of - 32.3 mV. The charged group content (COO- groups) in aCNFs was 1.5 mmol/g, comparable to that of cCNFs.

Dispersions containing 1 wt% CNFs presented highly viscous behavior, that demonstrated by inverted tube test (Fig. 2a and b). The morphology of the CNFs was analyzed by AFM, which showed that both cCNF and aCNF samples presented individually dispersed nanofibrils (Fig. 2c and d), with diameters of approximately 2 nm (Fig. 2e–g).

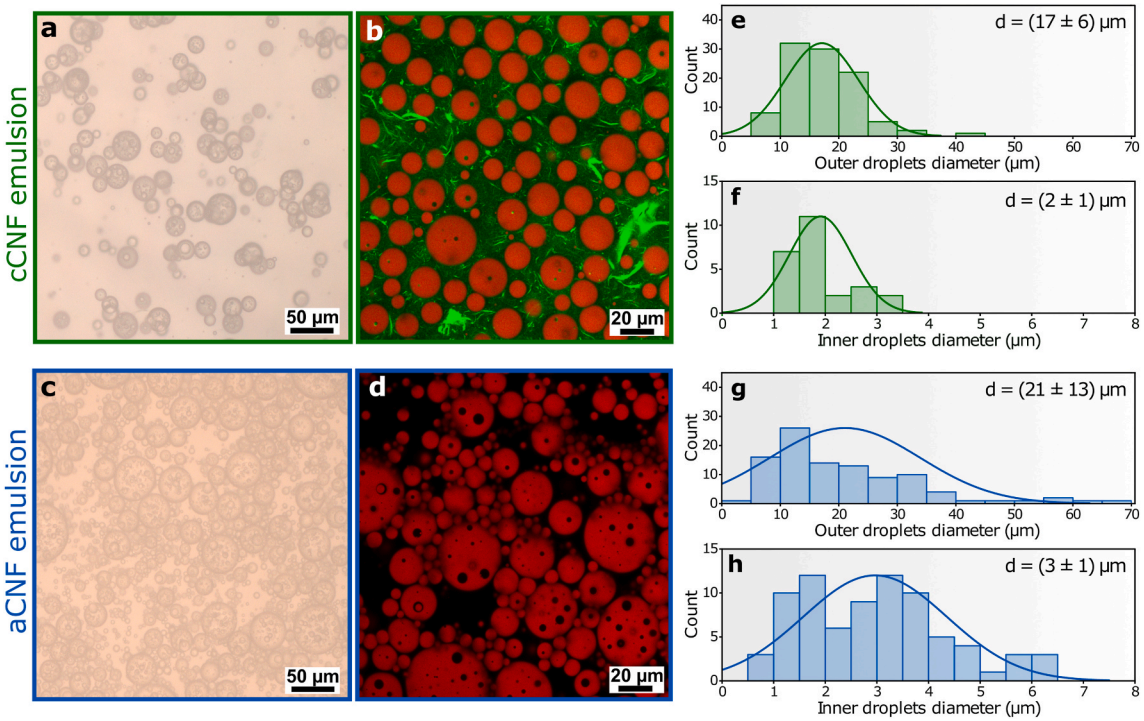


**Fig. 4.** Optical and CLSM images of freshly prepared (a,b) cCNF and (c,d) aCNF emulsions, respectively. The oil phase is shown in red, and the water phase in green. Outer and inner droplet size distribution histograms of (e,f) cCNF and (g,h) aCNF emulsions, displaying the average and standard deviation. (For interpretation of the references to colour in this figure legend, the reader is referred to the Web version of this article.)

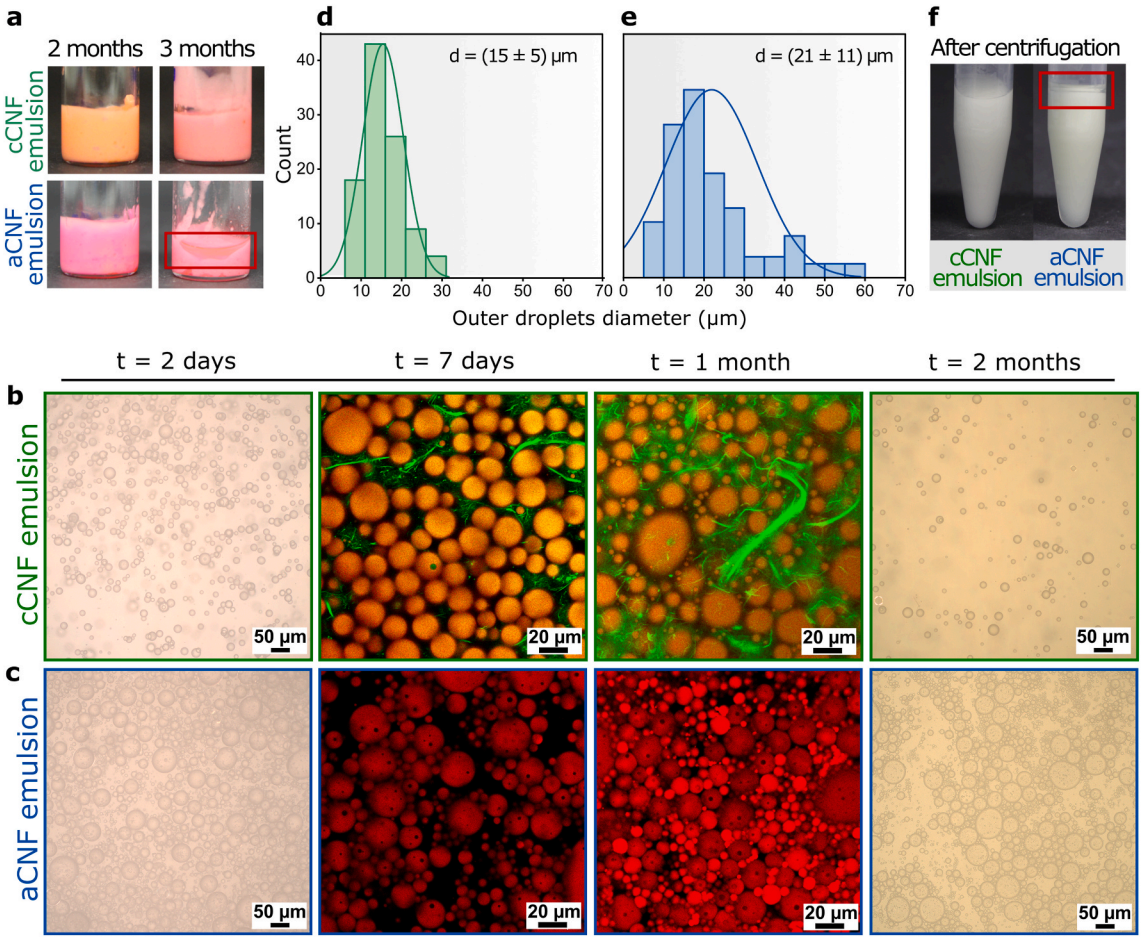


**Fig. 5.** (a) Photographs of cCNF and aCNF emulsions dyed with Nile red and fluorescein after 2 and 3 months of storage. Optical and CLSM micrographs of (b) cCNF and (c) aCNF emulsions as a function of storage time (2 days, 7 days, 1 month, and 2 months). Outer droplet size distribution histograms of (d) cCNF and (e) aCNF emulsions after 2 months of storage. (f) Photographs of cCNF and aCNF emulsions after centrifugation. The red boxes in (a,f) indicate the release of oil from the emulsions. (For interpretation of the references to colour in this figure legend, the reader is referred to the Web version of this article.)

Comparing nanofibrils lengths, cCNFs had relatively shorter fibrils with an aspect ratio (L/d) of about 100, while aCNFs displayed a higher aspect ratio of about 150 (Fig. 2f–h). The visual appearance of the CNF dispersions (Fig. 2a and b) showed that cCNF dispersion was more turbid than the aCNF dispersion. SEM images (Fig. S1) showed microfibrils within the nanofibril network in both samples. However, cCNF images revealed microfibrils with larger diameters, which likely accounts for the increased turbidity observed in their dispersion.

### 3.2. *Preparation and morphology of $W_1/O/W_2$ multiple emulsions*

Multiple emulsions were prepared using almond oil and 1 wt% aqueous dispersions of cCNFs or aCNFs, with an oil/water ratio of 40/60, through a one-step emulsification procedure (Fig. 3a). The emulsification was carried out using a high-speed blender at 30,000 rpm for 5 min. As shown in Fig. 3b, the resulting emulsions exhibited a uniform appearance with no visible macroscopic phase separation. Dilution tests demonstrated that the emulsions could be dispersed in water, confirming that water was the outer continuous phase in both emulsions, consistent with the hydrophilic nature of the nanocelluloses.

Optical micrographs of the emulsions revealed the presence of larger droplets encapsulating smaller ones, confirming the formation of multiple emulsions, as shown in Fig. 4a and c. To further confirm this microstructure, confocal laser scanning microscopy (CLSM) was performed using fluorescein disodium salt and Nile red to stain the aqueous (green) and oil (red) phases, respectively. The micrographs in Fig. 4b and d showed that water droplets were encapsulated within oil droplets, confirming the formation of water-in-oil-in-water ($W_1/O/W_2$) multiple emulsions for both cCNF and aCNF systems. Cryogenic transmission electron microscopy (cryo-TEM) imaging provided additional structural evidence of the multiple emulsion morphology, demonstrating the presence of internal aqueous droplets in the oil phase of the cCNF emulsion (Fig. S2).

Analysis of droplet size distribution revealed that both cCNF and aCNF emulsions featured outer oil droplets with diameters in tens of micrometers, encapsulating inner water droplets of a few micrometers wide (Fig. 4e–h). Despite similar structures among the emulsions, the cCNF emulsion exhibited smaller outer and inner droplets compared to the aCNF emulsion. Moreover, the droplet size distribution of the aCNF emulsion was broader, corresponding to a less uniform system.

### 3.3. *Stabilization of the $W_1/O/W_2$ multiple emulsions*

Instability is the main challenge in designing multiple emulsions, primarily due to the presence of two thermodynamically unstable interfaces (Cunha et al., 2014). The adsorption of colloidal particles at liquid-liquid interfaces, which reduces the interfacial free energy, is a key mechanism for the stabilization of Pickering emulsions. Another important mechanism is the formation of a particle network within the continuous phase, which increases the viscosity and reduces droplet mobility and coalescence (Sarkar & Dickinson, 2020). In this study, cCNFs and aCNFs, were evaluated as Pickering stabilizers for the

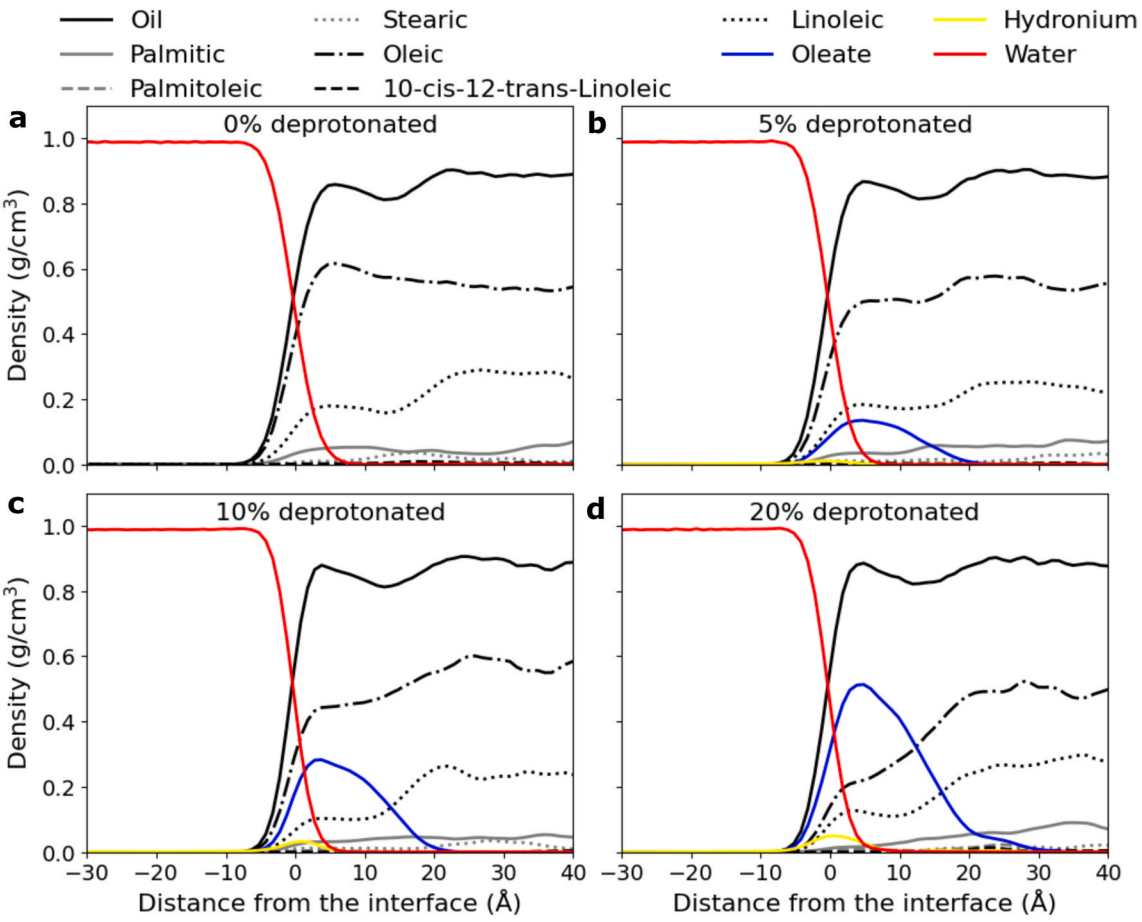


**Fig. 6.** Partitioned density profiles normal to the oil-water interface for the simulated systems with different deprotonation degrees of oleic acid: (a) 0%, (b) 5%, (c) 10% and (d) 20%.

oil–water ($O/W_2$) interface in our multiple emulsions.

The colloidal stability of the outer oil droplets was assessed by monitoring the visual appearance and morphology of the emulsions over time. The multiple emulsions stabilized either by cCNFs or aCNFs exhibited remarkable resistance to creaming and oiling off, with no macroscopic phase separation even after two months of storage (Fig. 5a). Optical microscopy and CLSM (Fig. 5b–c) confirmed the preservation of the oil droplets' morphology and showed no significant changes in the average size after two months (Fig. 5d–e). This reveals that cCNF and aCNFs can effectively stabilize the external oil droplets against coalescence and Ostwald ripening within two months of storage.

Just after three months, aCNF stabilized emulsions showed signs of macroscopic phase separation, suggesting lower colloidal stability compared to cCNF emulsions (Fig. 5a). Centrifugation tests (Fig. 5f) further confirmed this behavior, revealing significant phase separation in aCNF emulsions. This phenomenon, known as oiling off, arises from the coalescence and migration of oil droplets into a continuous oil layer, reflecting poorer droplet stabilization by the negatively charged nanofibrils (Myers, 1999, chap. 11). Oil droplets usually exhibit an intrinsically negative net charge due to the accumulation of negative groups at hydrophobic/water interfaces (Roger & Cabane, 2012). Therefore, the lower stability of aCNF emulsions can be attributed to electrostatic repulsion between the negatively charged oil droplets and the carboxylate groups of aCNF, which hinders effective particle adsorption at the oil-water interface.

In contrast, cCNF-stabilized emulsions exhibited higher stability, in agreement with previous studies (Shin et al., 2025; Silva et al., 2020). Silva et al. (Silva et al., 2020) demonstrated that cationic CNF-stabilized O/W emulsions with almond oil present greater resistance to coalescence compared to those stabilized by anionic CNFs. This enhanced stability was attributed to the increased viscosity of the continuous phase and attractive electrostatic interactions between the cationic groups of CNFs and negatively charged oil droplets. The additional negative charge of the oil phase arises from the presence of deprotonated free oleic acid in almond oil (0.1 wt%, see Table S1), favoring cCNF adsorption at the interface. This mechanism explains the relatively superior long-term and centrifugation stability of cCNF emulsion. Similar findings were reported by Shin et al. (Shin et al., 2025). They observed that in O/W emulsions with n-decane as the oil phase, cationic CNFs self-assemble into robust networks in oil droplets through attractive electrostatic interactions. They also reported a reduction in interfacial tension for oils with higher negative charge densities, such as oleic acid, demonstrating the preferential adsorption of cationic groups at more negatively charged interfaces.

The internal water droplets ($W_1/O$) in the multiple emulsions were formed without the use of an additional lipophilic emulsifier, which is usually required in such systems. Given the high hydrophilicity of the CNFs employed here, they are unlikely to stabilize the inner $W_1/O$ interface. This strongly suggests that a naturally occurring component in almond oil is responsible for stabilizing the $W_1/O$ emulsion. Besides, as shown in Fig. 5b–c, the type of CNF had a pronounced effect on the stability of the inner water droplets. In cCNF emulsions, most internal droplets disappeared within a few days, whereas aCNF emulsions maintained them for over two months, with an average diameter of ($3 \pm 1$) μm. These results demonstrate that, although cCNFs are more effective in stabilizing the outer oil droplets, the emulsion containing aCNFs is superior in preserving the internal water phase. This difference may arise from opposite electrostatic interactions between the CNF types and

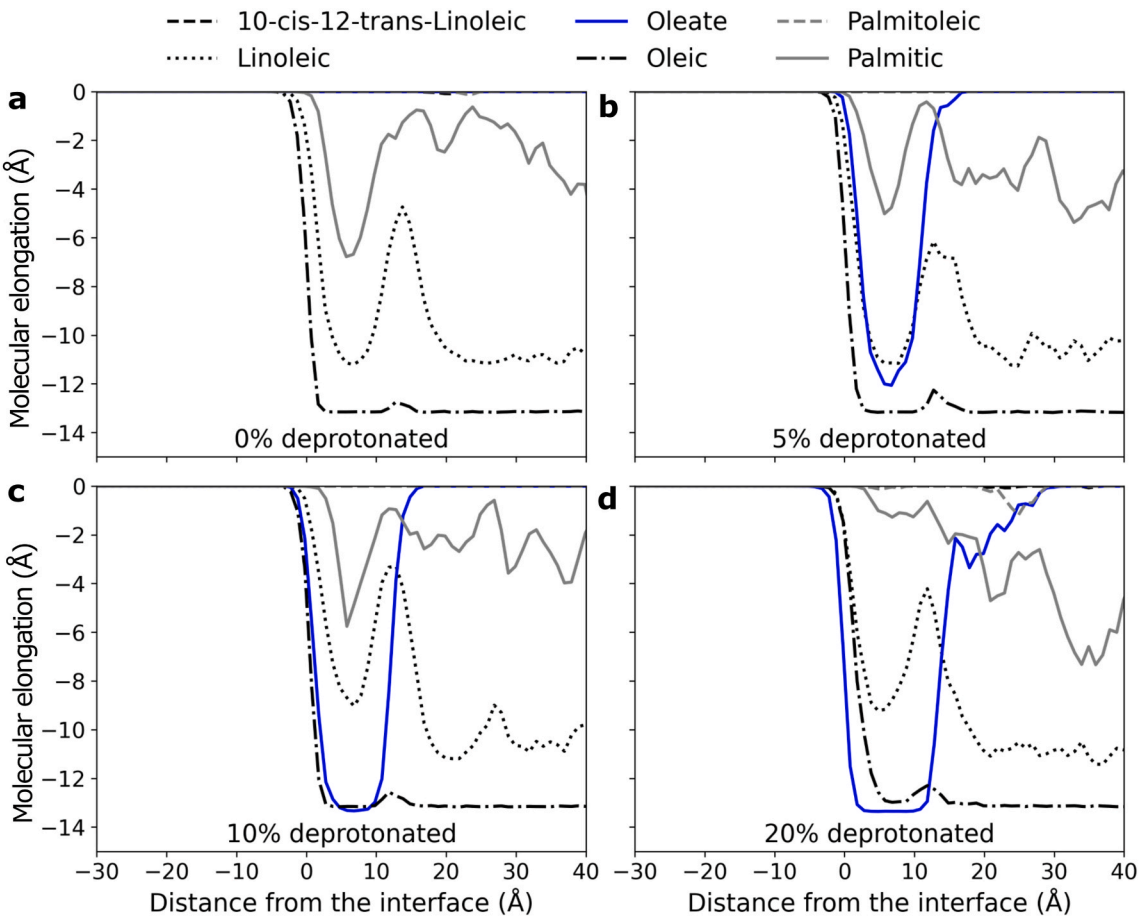


**Fig. 7.** Molecular elongation of the different molecules in the oil for the simulated systems with different deprotonation degrees of oleic acid: (a) 0%, (b) 5%, (c) 10% and (d) 20%.

the hydrophobic stabilizer, which affect the stability of water droplets.

### 3.4. Oleic acid at the water-oil ($W_1/O$) interface

Despite differences in stability, the systems containing cCNF or aCNF as added stabilizers were able to form multiple emulsions in a single step. The formation of water droplets, without the addition of hydrophobic emulsifiers, suggests that a component within the almond oil plays a role in stabilizing these droplets. Almond oil is a complex vegetable oil, mainly composed of lipids, particularly fatty acids (FA) ranging from C14 to C20, including saturated, monounsaturated, and polyunsaturated chains. Among these, oleic acid is the main FA (43.3-81.5%) (Ouzir et al., 2021). Natural oils also contain a fraction of free fatty acids (FFA) derived from triglyceride hydrolysis (Mohammed & Ikiensikimama, 2023), typically ranging from 0.05 to 0.70 wt % in commercial oils, which is commonly referred to as oil acidity (Waraho et al., 2011). The interfacial properties of FAs have been previously reported in systems such as foams (Shu et al., 2014) and emulsions (Freire et al., 2022).

To assess the role of FAs in multiple emulsion formation, the FA profile and FFA content of the almond oil used were analyzed. The composition was consistent with literature (Ouzir et al., 2021), with oleic acid as the major FA (67.57%) (see Table S1). The almond oil had an acidity of 0.1 wt%, which was attributed to free oleic acid due to its high abundance. The FA profile obtained here is similar to previous studies of almond oil in O/W emulsions stabilized with cCNFs, as described by Silva et al. (Silva et al., 2020). However, the study used almond oil with a lower acidity (0.03 wt %), revealing that the higher free oleic acid content in the present work may play a role in the formation of multiple emulsions. In previous studies, when oleic acid was employed as an emulsion stabilizer, it was most often combined with its ionized form, oleate, to promote the stabilization of O/W emulsions (Freire et al., 2022). In contrast, oleic acid in its protonated form exhibits a low HLB, which enables it to act as a potential W/O emulsifier (Myers, 1999, chap. 11; Pasquali et al., 2008).

To further investigate the influence of FFAs in multiple emulsions formation, Pickering emulsions were prepared in one-step using mineral oil as a model oil, and aCNF as stabilizer. In this case, stable simple O/W emulsions were obtained, but no multiple emulsions were formed, confirming that the oil composition plays a key role in determining the multiple morphology (Fig. S2). Similar results were reported by Li et al. (Y. Li, Gong, et al., 2021), who demonstrated that temporary multiple emulsions could be formed using CNCs and soybean oil in a single step. However, only simple emulsions were formed when pure oils, such as toluene, were used. They hypothesized that surface-active compounds present in the soybean oil influence the preparation of multiple emulsions.

The ability of almond oil components to stabilize W/O emulsions was directly assessed by preparing mixtures of almond oil-water mixtures (99:1, oil/water) without any added emulsifiers (Fig. S3a). Microscopy confirmed the formation of W/O emulsions under these conditions. An analogous experiment using pure oleic acid yielded W/O emulsions (Fig. S3b), although with lower stability than those formed with almond oil, suggesting a synergistic contribution of the FA mixture naturally present in almond oil (Posocco et al., 2016; Rosen & Kunjappu, 2012; Zhou et al., 2014).

MD simulations are an effective approach for overcoming experimental limitations by providing molecular-level insights into the oil-

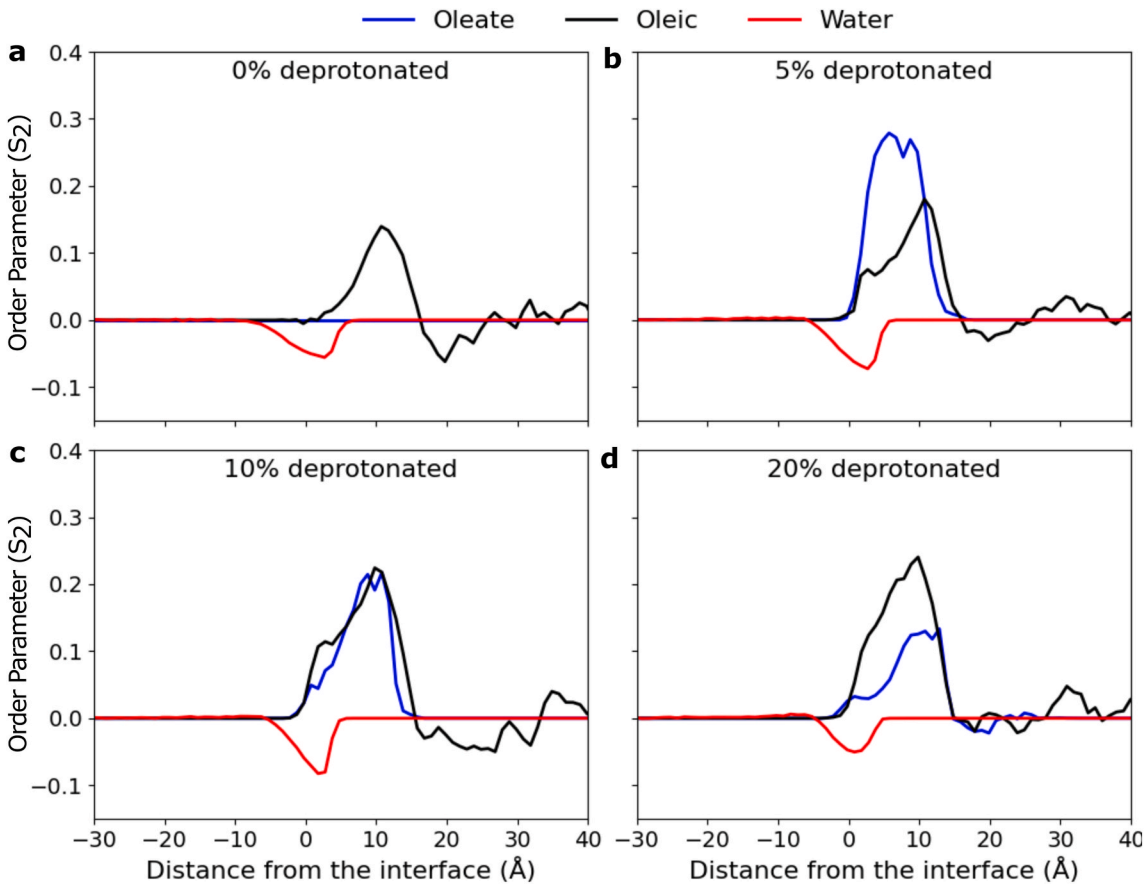


**Fig. 8.** Order parameter ($S_2$) of oleic acid, oleate, and water for the simulated systems with different deprotonation degrees of oleic acid: (a) 0%, (b) 5%, (c) 10% and (d) 20%.

water interface behavior (Muhammad et al., 2024). In this study, classical MD simulations were used to characterize the interfacial properties of FFAs individually. Four systems with varying degrees of oleic acid deprotonation (0%, 5%, 10%, and 20%) were investigated, while maintaining a constant composition of the remaining components. This enabled the systematic evaluation of interfacial effects that cannot be directly accessed through experimental measurements alone. Mono-, di, and triglycerides were excluded from the simulations, as FFAs predominate at the interface region due to their higher surface activity.

Density profiles normal to the interface (Fig. 6) showed that oleic acid preferentially accumulates at the interface when the deprotonation degree is 0%, indicating that oleic acid is the FFA with the strongest surface activity in almond oil. As deprotonation increases, oleate ions accumulate more at the interface, raising the charge density (Fig. S4). Additionally, moving toward the bulk phase, the oleate density declines sharply, reflecting the bulkier nature of protonated FFAs compared to oleate. The increased hydrophilicity of the carboxylate groups in oleate explains its stronger interfacial adsorption compared to protonated FFAs.

Molecular elongation analysis was conducted to describe the shape of the conformational distribution of the adsorbed molecules, offering insight into their organization at the interface. Elongated molecules display values near zero, while contracted conformations yield negative values. The molecular elongation values for FFAs (Fig. 7), ranging from approximately zero near the interface to negative further away, demonstrate that the FFAs are predominantly elongated in the interfacial region and adopt more compact or disordered conformations away from it.

Additional insights into molecular orientation were obtained using the order parameter $S_2$ (Fig. 8). An $S_2$ value of 1 signifies molecules are fully perpendicular to the interface, while $S_2 = -1/2$ corresponds to all molecules being parallel to the interface. Randomly oriented molecules yield $S_2 = 0$ (Müller et al., 2021). Near the interface, oleic acid and oleate exhibit a preferential orientation due to hydrogen bonding with water, resulting in a lower angle of their polar head with respect to the normal to the interface and a higher $S_2$ value. Together with the molecular elongation analysis, one can say the whole molecule is oriented perpendicular to the interface. Increasing the deprotonation reduced the $S_2$ of oleate, likely due to repulsion, while slightly increasing the orientation of protonated oleic acid, possibly as a response to mitigate repulsion effects.

Computational calculations of interfacial tension (IFT) (Fig. 9a) revealed a progressive decrease from 28 to 19 mN $m^{-1}$ as the deprotonation degree decreased from 20% to 0%. The accumulation of oleate at the interface increases the negative local charge density (Fig. S4), which leads to electrostatic repulsion and, consequently, a higher IFT. Conversely, higher concentrations of protonated oleic acid (i.e., lower pH) resulted in lower IFT, favoring the stabilization of water-in-oil (W/O) droplets and thereby enabling the formation of multiple emulsions. Overall, these findings show that oleic acid plays a primary role in interfacial stabilization of inner water droplets. Other FAs, with different chain lengths and degrees of unsaturation, may contribute synergistically, as evidenced by the greater stability of W/O emulsions formed with almond oil compared to those prepared with pure oleic acid. The values of IFT obtained here from MD simulations agree with the experimental results of the water-almond oil IFT from the literature (22-24 mN/m) (Silva et al., 2020).

This work reveals a stabilization mechanism in one-step $W_1/O/W_2$ multiple emulsions. CNFs mainly act at the outer oil–water interface ($O/W_2$), where their adsorption and the concomitant increase in

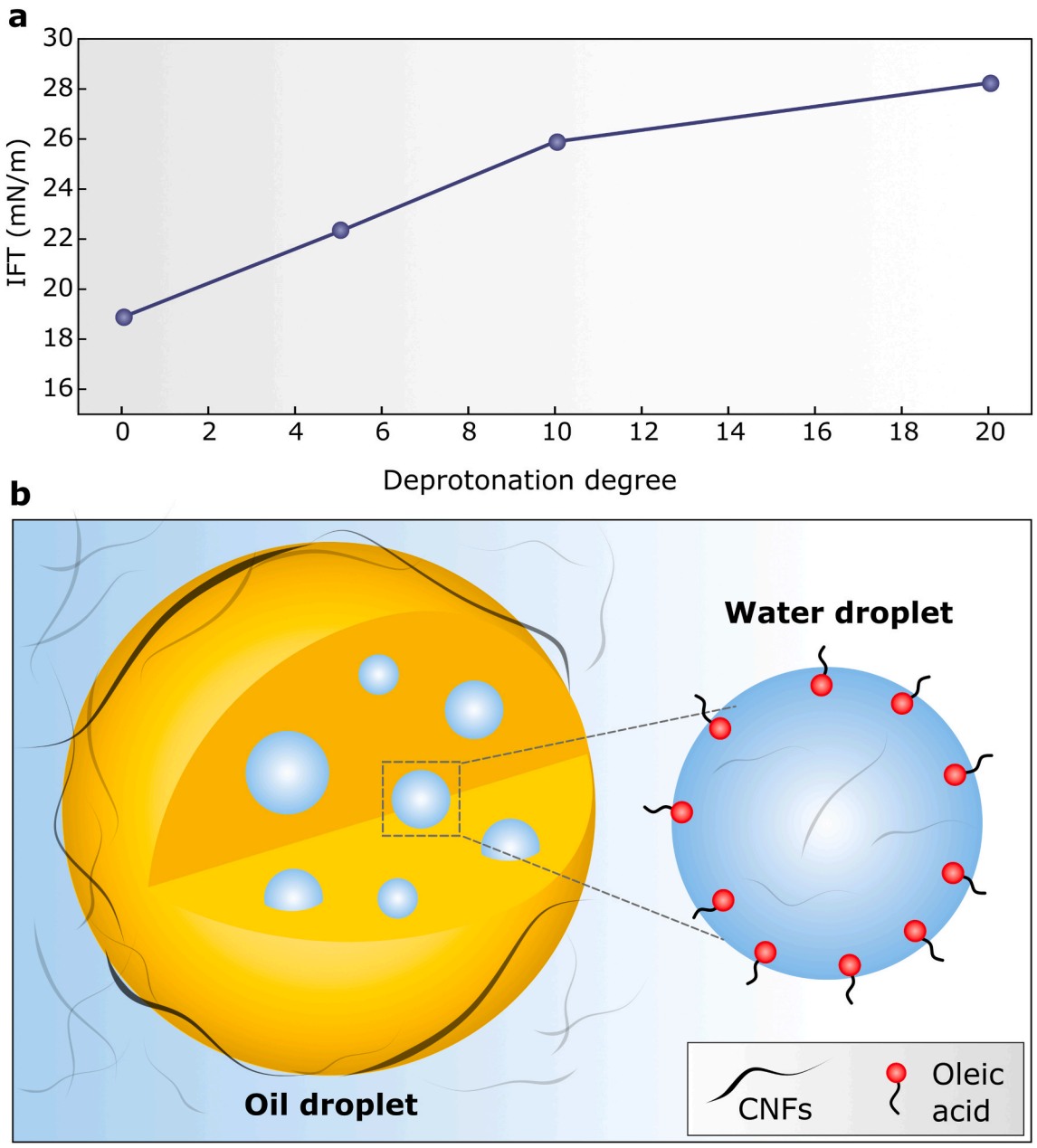


**Fig. 9.** (a) Interfacial tension (IFT) values as a function of the deprotonation degree of oleic acid. (b) Schematic representation of the stabilization mechanism in $W_1/O/W_2$ multiple emulsions.

continuous-phase viscosity hinder oil droplet coalescence. In parallel, the combined experimental and computational analysis demonstrated that free oleic acid in almond oil is responsible for stabilizing the internal water-in-oil droplets ($W_1/O$) (Fig. 9b), and is effective at concentrations as low as 0.1 wt% (Garti, 1997). The longer preservation of multiple morphology in aCNF-based emulsions compared with cCNF-based ones can be rationalized by the electrostatic repulsion between oleic acid and aCNFs, which maintains a higher fraction of oleic acid available to stabilize the internal droplets. Altogether, these findings delineate a clear division of function between CNFs and oleic acid in the stabilization of the multiple emulsion structure.

## 4. Conclusions

This work demonstrates that functionalized cellulose nanofibrils and oleic acid can be used as stabilizers to formulate bio-based $W_1/O/W_2$ multiple emulsions through a one-step process. Cationic and anionic cellulose nanofibrils (cCNFs and aCNFs) effectively stabilized the oil droplets ($O/W_2$) by increasing the viscosity of the continuous phase. In cCNF-based systems, stabilization was further enhanced by electrostatic attraction between positively charged nanofibrils and negatively charged oil droplets. The internal water droplets ($W_1/O$), in turn, were stabilized by oleic acid naturally present in almond oil, as evidenced by the inability of mineral oils to form multiple emulsions under identical conditions. Molecular dynamics simulations identified oleic acid as the most surface-active fatty acid at the interface, preferentially adopting an oriented and elongated conformation. A higher fraction of protonated oleic acid further lowered the interfacial tension, thereby promoting the formation of $W_1/O$ droplets. The CNF type was a critical factor governing the lifetime of the multiple structure, as emulsions stabilized with aCNFs retain their multiple morphology significantly longer than those with cCNFs. In contrast to previously reported two-step strategies (Garti & Bisperink, 1998), the approach presented here enables the simple generation of $W_1/O/W_2$ multiple emulsions in a single step.

Additionally, they rely exclusively on renewable stabilizers, avoiding the synthetic polymers and surfactants commonly used in the literature (Carrillo et al., 2015). Future studies could investigate the methodology with other natural oils containing free fatty acids. Furthermore, this work opens opportunities to develop multifunctional colloidal formulations for encapsulation and controlled release of bioactive substances (Muschiolik, 2007).

## CRediT authorship contribution statement

**Maria C.S. Oliveira:** Writing – review & editing, Writing – original draft, Validation, Methodology, Investigation, Formal analysis, Conceptualization. **Caroline E.P. Silva:** Writing – review & editing, Methodology, Conceptualization. **Elisa S. Ferreira:** Writing – review & editing, Methodology, Conceptualization. **James M. Almeida:** Writing – review & editing, Writing – original draft, Methodology, Investigation, Formal analysis, Conceptualization. **Juliana S. Bernardes:** Writing – review & editing, Supervision, Resources, Project administration, Methodology, Funding acquisition, Conceptualization.

## Declaration of generative AI and AI-assisted technologies in the writing process

During the preparation of this work, the authors used Grammarly, Microsoft Copilot, and ChatGPT to improve language clarity. After using this tool, the authors reviewed and edited the content as needed and assumed full responsibility for the final version of the published article.

## Declaration of competing interest

The authors declare that they have no known competing financial interests or personal relationships that could have appeared to influence the work reported in this paper.

## Acknowledgments

This research was supported by São Paulo Research FoundationSão Paulo Research Foundation (FAPESP, Grants No. 2024/20969-0, 2023/16370-3 and 2023/09659-7) and through the Research, Innovation and Dissemination Center for Molecular Engineering for Advanced Materials – CEMol (Grant CEPID No. 2024/00989-7). The authors also thank the staff from Biological Imaging Laboratory – LIB (LNBio, CNPEM), Atomic Force Microscopy Laboratory, and Scanning Electron Microscopy and Dual Beam Laboratory (LNNano, CNPEM) for technical support during microscopy images acquisition. The authors also thank Laura C. E. Silva from the Cryo-EM Laboratory (LNNano, CNPEM) for cryo-TEM image acquisition.

## Appendix A. Supplementary data

Supplementary data to this article can be found online at https://doi.org/10.1016/j.foodhyd.2026.112665.

## Data availability

Data will be made available on request.

## References

Aveyard, R., Binks, B. P., & Clint, J. H. (2003). Emulsions stabilised solely by colloidal particles. *Advances in Colloid and Interface Science, 100–102*, 503–546. https://doi.org/10.1016/S0001-8686(02)00069-6

Binks, B. P., & Horozov, T. S. (2006). *Colloidal particles at liquid interfaces*. Cambridge University Press (Chapter 1).

Carrillo, C. A., Nypelö, T. E., & Rojas, O. J. (2015). Cellulose nanofibrils for one-step stabilization of multiple emulsions (W/O/W) based on soybean oil. *Journal of Colloid and Interface Science, 445*, 166–173. https://doi.org/10.1016/j.jcis.2014.12.028

Case, D. A., Aktulga, H. M., Belfon, K., Cerutti, D. S., Cisneros, G. A., Cruzeiro, V. W. D., Forouzesh, N., Giese, T. J., Götz, A. W., Gohlke, H., Izadi, S., Kasavajhala, K., Kaymak, M. C., King, E., Kurtzman, T., Lee, T.-S., Li, P., Liu, J., Luchko, T., … Merz, K. M., Jr. (2023). AmberTools. *Journal of Chemical Information and Modeling, 63*(20), 6183–6191. https://doi.org/10.1021/acs.jcim.3c01153

Chau, P.-L., & Hardwick, A. J. (1998). A new order parameter for tetrahedral configurations. *Molecular Physics, 93*(3), 511–518. https://doi.org/10.1080/002689798169195

Choulis, N. H. (2011). Chapter 49—Miscellaneous drugs, materials, medical devices, and techniques. In J. K. Aronson (Ed.), *Side effects of drugs annual, 33* pp. 1009–1029). Elsevier. https://doi.org/10.1016/B978-0-444-53741-6.00049-0.

Cunha, A. G., Mougel, J.-B., Cathala, B., Berglund, L. A., & Capron, I. (2014). Preparation of double pickering emulsions stabilized by chemically tailored nanocelluloses. *Langmuir, 30*(31), 9327–9335. https://doi.org/10.1021/la5017577

de Almeida, T. M., de Almeida, J. M., Kudrna, K. B., Emanuelli, T., Leite, D. C., Frizzo, C. P., Paz, A. V., Schaffazick, S. R., de, B., & da Silva, C. (2023). Photostable ferulic acid-loaded nanoemulsion for anti-inflammatory skin application. *ACS Applied Nano Materials, 6*(24), 22807–22817. https://doi.org/10.1021/acsanm.3c03980

Dickson, C. J., Walker, R. C., & Gould, I. R. (2022). Lipid21: Complex lipid membrane simulations with AMBER. *Journal of Chemical Theory and Computation, 18*(3), 1726–1736. https://doi.org/10.1021/acs.jctc.1c01217

Dufresne, A. (2013). Nanocellulose: A new ageless bionanomaterial. *Materials Today, 16*(6), 220–227. https://doi.org/10.1016/j.mattod.2013.06.004

Freire, R. V. M., Haenni, E., Hong, L., Gontsarik, M., & Salentinig, S. (2022). Bioinspired oleic acid–triolein emulsions for functional material design. *Advanced Materials Interfaces, 9*(23), Article 2200446. https://doi.org/10.1002/admi.202200446

Fujisawa, S., Togawa, E., & Kuroda, K. (2017). Nanocellulose-stabilized pickering emulsions and their applications. *Science and Technology of Advanced Materials, 18*(1), 959–971. https://doi.org/10.1080/14686996.2017.1401423

Garti, N. (1997). Double emulsions—Scope, limitations and new achievements. *Colloids and Surfaces A: Physicochemical and Engineering Aspects, Frontiers in Colloid Chemistry an International Festschrift to Professor Stig E. Friberg, 123–124*, 233–246. https://doi.org/10.1016/S0927-7757(96)03809-5

Garti, N., & Bisperink, C. (1998). Double emulsions: Progress and applications. *Current Opinion in Colloid & Interface Science, 3*(6), 657–667. https://doi.org/10.1016/S1359-0294(98)80096-4

Götz, A. W., Williamson, M. J., Xu, D., Poole, D., Le Grand, S., & Walker, R. C. (2012). Routine microsecond molecular dynamics simulations with AMBER on GPUs. 1. Generalized born. *Journal of Chemical Theory and Computation, 8*(5), 1542–1555. https://doi.org/10.1021/ct200909j

Hąc-Wydro, K., & Wydro, P. (2007). The influence of fatty acids on model cholesterol/phospholipid membranes. *Chemistry and Physics of Lipids, 150*(1), 66–81. https://doi.org/10.1016/j.chemphyslip.2007.06.213

Irving, J. H., & Kirkwood, J. G. (1950). The statistical mechanical theory of transport processes. IV. The equations of hydrodynamics. *The Journal of Chemical Physics, 18*(6), 817–829. https://doi.org/10.1063/1.1747782

Isogai, A., Saito, T., & Fukuzumi, H. (2011). TEMPO-oxidized cellulose nanofibers. *Nanoscale, 3*(1), 71–85. https://doi.org/10.1039/C0NR00583E

Johansson, I., & Svensson, M. (2001). Surfactants based on fatty acids and other natural hydrophobes. *Current Opinion in Colloid & Interface Science, 6*(2), 178–188. https://doi.org/10.1016/S1359-0294(01)00076-0

Jorgensen, W. L., Chandrasekhar, J., Madura, J. D., Impey, R. W., & Klein, M. L. (1983). Comparison of simple potential functions for simulating liquid water. *The Journal of Chemical Physics, 79*(2), 926–935. https://doi.org/10.1063/1.445869

Kamogawa, K., Akatsuka, H., Matsumoto, M., Yokoyama, S., Sakai, T., Sakai, H., & Abe, M. (2001). Surfactant-free O/W emulsion formation of oleic acid and its esters with ultrasonic dispersion. *Colloids and Surfaces A: Physicochemical and Engineering Aspects, 180*(1), 41–53. https://doi.org/10.1016/S0927-7757(00)00758-5

Kamogawa, K., Okudaira, G., Matsumoto, M., Sakai, T., Sakai, H., & Abe, M. (2004). Preparation of oleic acid/water emulsions in surfactant-free condition by sequential processing using Midsonic−Megasonic waves. *Langmuir, 20*(6), 2043–2047. https://doi.org/10.1021/la030160z

Li, Y., Gong, S., Guan, X., Jiang, H., Tao, S., Yang, C., & Ngai, T. (2021). One-step preparation of all-natural pickering double emulsions stabilized by oppositely charged biopolymer particles. *Advanced Materials Interfaces, 8*(23), Article 2101568. https://doi.org/10.1002/admi.202101568

Li, P., Song, L. F., & Merz, K. M., Jr. (2015). Systematic parameterization of monovalent ions employing the nonbonded model. *Journal of Chemical Theory and Computation, 11*(4), 1645–1657. https://doi.org/10.1021/ct500918t

Li, Q., Wu, Y., Fang, R., Lei, C., Li, Y., Li, B., Pei, Y., Luo, X., & ShilinLiu. (2021). Application of Nanocellulose as particle stabilizer in food pickering emulsion: Scope, Merits and challenges. *Trends in Food Science & Technology, 110*, 573–583. https://doi.org/10.1016/j.tifs.2021.02.027

Lu, T. (2024). A comprehensive electron wavefunction analysis toolbox for chemists, Multiwfn. *The Journal of Chemical Physics, 161*(8), Article 082503. https://doi.org/10.1063/5.0216272

Lu, T., & Chen, F. (2012). Multiwfn: A multifunctional wavefunction analyzer. *Journal of Computational Chemistry, 33*(5), 580–592. https://doi.org/10.1002/jcc.22885

Martínez, L., Andrade, R., Birgin, E. G., & Martínez, J. M. (2009). PACKMOL: A package for building initial configurations for molecular dynamics simulations. *Journal of Computational Chemistry, 30*(13), 2157–2164. https://doi.org/10.1002/jcc.21224

Miyamoto, S., & Kollman, P. A. (1992). Settle: An analytical version of the SHAKE and RATTLE algorithm for rigid water models. *Journal of Computational Chemistry, 13*(8), 952–962. https://doi.org/10.1002/jcc.540130805

Mohammed, S., & Ikiensikimama, S. S. (2023). Vegetable oils as surfactant feedstocks for enhanced oil recovery: A review. *Chemical Engineering Research and Design, 200*, 693–705. https://doi.org/10.1016/j.cherd.2023.11.011

Morais, J. M., Rocha-Filho, P. A., & Burgess, D. J. (2009). Influence of phase inversion on the formation and stability of one-step multiple emulsions. *Langmuir, 25*(14), 7954–7961. https://doi.org/10.1021/la9007125

Muhammad, A. H., Asma, M., Hamed, Y. S., Hameed, A., Abdullah, J. W., Peilong, S., Kai, Y., & Ming, C. (2024). Enhancing cellulose-stabilized multiphase/Pickering emulsions systems: A molecular dynamics perspective. *International Journal of Biological Macromolecules, 277*, Article 134244. https://doi.org/10.1016/j.ijbiomac.2024.134244

Müller, P., Bonthuis, D. J., Miller, R., & Schneck, E. (2021). Ionic surfactants at air/water and oil/water interfaces: A comparison based on molecular dynamics simulations. *The Journal of Physical Chemistry B, 125*(1), 406–415. https://doi.org/10.1021/acs.jpcb.0c08615

Muschiolik, G. (2007). Multiple emulsions for food use. *Current Opinion in Colloid & Interface Science, 12*(4), 213–220. https://doi.org/10.1016/j.cocis.2007.07.006

Myers, D. (1999). *Surfaces, interfaces, and colloids* (2nd ed.). New York: Wiley (Chapter 11).

Neese, F. (2012). The ORCA program system. *WIREs Computational Molecular Science, 2*(1), 73–78. https://doi.org/10.1002/wcms.81

Neese, F. (2022). Software update: The ORCA program system—Version 5.0. *WIREs Computational Molecular Science, 12*(5), Article e1606. https://doi.org/10.1002/wcms.1606

Niu, H., Wang, W., Dou, Z., Chen, X., Chen, X., Chen, H., & Fu, X. (2023). Multiscale combined techniques for evaluating emulsion stability: A critical review. *Advances in Colloid and Interface Science, 311*, Article 102813. https://doi.org/10.1016/j.cis.2022.102813

Ouzir, M., Bernoussi, S. E., Tabyaoui, M., & Taghzouti, K. (2021). Almond oil: A comprehensive review of chemical composition, extraction methods, preservation conditions, potential health benefits, and safety. *Comprehensive Reviews in Food Science and Food Safety, 20*(4), 3344–3387. https://doi.org/10.1111/1541-4337.12752

Pasquali, R. C., Taurozzi, M. P., & Bregni, C. (2008). Some considerations about the hydrophilic–lipophilic balance system. *International Journal of Pharmaceutics, 356*(1), 44–51. https://doi.org/10.1016/j.ijpharm.2007.12.034

Posocco, P., Perazzo, A., Preziosi, V., Laurini, E., Pricl, S., & Guido, S. (2016). Interfacial tension of oil/water emulsions with mixed non-ionic surfactants: Comparison between experiments and molecular simulations. *RSC Advances, 6*(6), 4723–4729. https://doi.org/10.1039/C5RA24262B

Roger, K., & Cabane, B. (2012). Why are hydrophobic/water interfaces negatively charged? *Angewandte Chemie International Edition, 51*(23), 5625–5628. https://doi.org/10.1002/anie.201108228

Rosen, M. J., & Kunjappu, J. T. (2012). *Surfactants and interfacial phenomena*. John Wiley & Sons.

S Clegg, P., W Tavacoli, J., & J Wilde, P. (2016). One-step production of multiple emulsions: Microfluidic, polymer-stabilized and particle-stabilized approaches. *Soft Matter, 12*(4), 998–1008. https://doi.org/10.1039/C5SM01663K

Saito, T., Kimura, S., Nishiyama, Y., & Isogai, A. (2007). Cellulose nanofibers prepared by TEMPO-mediated oxidation of native cellulose. *Biomacromolecules, 8*(8), 2485–2491. https://doi.org/10.1021/bm0703970

Salomon-Ferrer, R., Götz, A. W., Poole, D., Le Grand, S., & Walker, R. C. (2013). Routine microsecond molecular dynamics simulations with AMBER on GPUs. 2. Explicit solvent particle mesh ewald. *Journal of Chemical Theory and Computation, 9*(9), 3878–3888. https://doi.org/10.1021/ct400314y

Sarkar, A., & Dickinson, E. (2020). Sustainable food-grade pickering emulsions stabilized by plant-based particles. *Current Opinion in Colloid & Interface Science, Emulsions and Microemulsions, 49*, 69–81. https://doi.org/10.1016/j.cocis.2020.04.004

Shi, P., Zhang, H., Lin, L., Song, C., Chen, Q., & Li, Z. (2018). Molecular dynamics simulation of four typical surfactants at oil/water interface. *Journal of Dispersion Science and Technology, 39*(9), 1258–1265. https://doi.org/10.1080/01932691.2017.1392319

Shin, J., Seo, B., Choi, K., Park, D., Lee, H. J., Kim, H., Shin, D., Park, B. J., & Kim, J. W. (2025). Charge-directed nanocellulose assembly for interfacial phase-transfer catalysis. *Advanced Materials, 37*(17), Article 2418325. https://doi.org/10.1002/adma.202418325

Shu, X., Meng, Y., Wan, L., Li, G., Yang, M., & Jin, W. (2014). pH-Responsive aqueous foams of oleic acid/oleate solution. *Journal of Dispersion Science and Technology, 35*(2), 293–300. https://doi.org/10.1080/01932691.2013.785363

Sieben, P. G., Wypych, F., & de Freitas, R. A. (2022). Oleic acid as a synergistic agent in the formation of kaolinite-mineral oil pickering emulsions. *Applied Clay Science, 216*, Article 106378. https://doi.org/10.1016/j.clay.2021.106378

Silva, C. E. P., Tam, K. C., Bernardes, J. S., & Loh, W. (2020). Double stabilization mechanism of O/W pickering emulsions using cationic nanofibrillated cellulose. *Journal of Colloid and Interface Science, 574*, 207–216. https://doi.org/10.1016/j.jcis.2020.04.001

Suga, K., Kondo, D., Otsuka, Y., Okamoto, Y., & Umakoshi, H. (2016). Characterization of aqueous oleic acid/oleate dispersions by fluorescent probes and raman spectroscopy. *Langmuir, 32*(30), 7606–7612. https://doi.org/10.1021/acs.langmuir.6b02257

Svensson, M. (2010). Surfactants based on natural fatty acids. In *Surfactants from renewable resources* (pp. 1–19). John Wiley & Sons, Ltd. https://doi.org/10.1002/9780470686607.ch1.

Waraho, T., McClements, D. J., & Decker, E. A. (2011). Impact of free fatty acid concentration and structure on lipid oxidation in oil-in-water emulsions. *Food Chemistry, 129*(3), 854–859. https://doi.org/10.1016/j.foodchem.2011.05.034

Woods, R. J., & Chappelle, R. (2000). Restrained electrostatic potential atomic partial charges for condensed-phase simulations of carbohydrates. *Journal of Molecular Structure: THEOCHEM, 527*(1), 149–156. https://doi.org/10.1016/S0166-1280(00)00487-5

Zakir Hossain, K. M., Deeming, L., & Edler, K. J. (2021). Recent progress in pickering emulsions stabilised by bioderived particles. *RSC Advances, 11*(62), 39027–39044. https://doi.org/10.1039/D1RA08086E

Zaman, M., Xiao, H., Chibante, F., & Ni, Y. (2012). Synthesis and characterization of cationically modified nanocrystalline cellulose. *Carbohydrate Polymers, 89*(1), 163–170. https://doi.org/10.1016/j.carbpol.2012.02.066

Zhao, H., Yang, Y., Chen, Y., Li, J., Wang, L., & Li, C. (2022). A review of multiple pickering emulsions: Solid stabilization, preparation, particle effect, and application. *Chemical Engineering Science, 248*, Article 117085. https://doi.org/10.1016/j.ces.2021.117085

Zhou, Z.-H., Zhang, Q., Liu, Y., Wang, H.-Z., Cai, H.-Y., Zhang, F., Tian, M.-Z., Liu, Z.-Y., Zhang, L., & Zhang, L. (2014). Effect of fatty acids on interfacial tensions of novel sulfobetaines solutions. *Energy & Fuels, 28*(2), 1020–1027. https://doi.org/10.1021/ef402416j